

Teleconnections between Ethiopian rainfall variability and global SSTs: observations and methods for model evaluation

Mekonnen Adnew Degefu¹ · David P. Rowell² · Woldeamlak Bewket¹

Received: 27 May 2015 / Accepted: 31 May 2016 / Published online: 27 June 2016
© The Author(s) 2016. This article is published with open access at Springerlink.com

Abstract Rainfall variability in Ethiopia has significant effects on rainfed agriculture and hydropower, so understanding its association with slowly varying global sea surface temperatures (SSTs) is potentially important for prediction purposes. We provide an overview of the seasonality and spatial variability of these teleconnections across Ethiopia. A quasi-objective method is employed to define coherent seasons and regions of SST-rainfall teleconnections for Ethiopia. We identify three seasons (March–May, MAM; July–September, JAS; and October–November, ON), which are similar to those defined by climatological rainfall totals. We also identify three new regions (Central and western Ethiopia, CW-Ethiopia; Southern Ethiopia, S-Ethiopia; and Northeast Ethiopia, NE-Ethiopia) that are complementary to those previously defined here based on distinct SST-rainfall teleconnections that are useful when predicting interannual anomalies. JAS rainfall over CW-Ethiopia is negatively associated with SSTs over the equatorial east Pacific and Indian Ocean. New regional detail is added to that previously found for the whole of East Africa, in particular that ON rainfall over

S-Ethiopia is positively associated with equatorial east Pacific SSTs and with the Indian Ocean Dipole (IOD). Also, SST-to-rainfall correlations for other season-regions, and specifically for MAM in all regions, are found to be negligible. The representation of these teleconnections in the HadGEM2 and HadGEM3-GA3.0 coupled climate models shows mixed skill. Both models poorly represent the statistically significant teleconnections, except that HadGEM2 and the low resolution (N96) version of HadGEM3-GA3.0 better represent the association between the IOD and S-Ethiopian ON rainfall. Additionally, both models are able to represent the lack of SST-rainfall correlation in other seasons and other parts of Ethiopia.

1 Introduction

Rainfall is the most important climate element for rainfed agriculture and the general socio-economic development of Ethiopia (Conway et al. 2011). Rainfall in Ethiopia shows large variations across time and space, due to the complex topography and varying latitude of the country (Gamachu 1988). Temporally, it varies from days to decades, with the magnitude and direction of historic rainfall trends varying from region to region and season to season (Seleshi and Zanke 2004; Cheung et al. 2008; Jury and Funk 2012; Viste and Sorteberg 2013). Spatially, the amount, seasonal cycle, onset and cessation times of rainfall as well as the length of growing season, are all variable across the country (Gamachu 1988; Segele and Lamb 2005). This complex spatio-temporal variability of rainfall over Ethiopia is attributed to the large variations in altitude (Gamachu 1988), variations in sea surface temperatures (SSTs) over the Indian, Pacific and Atlantic Oceans (e.g. Korecha and Barnston 2007;

Responsible Editor: J. T. Fasullo.

✉ Mekonnen Adnew Degefu
mekonnenadnew@yahoo.com

David P. Rowell
dave.rowell@metoffice.gov.uk

Woldeamlak Bewket
wbewket@yahoo.com

¹ Department of Geography and Environmental Studies, Addis Ababa University, P.O. Box: 1176, Addis Ababa, Ethiopia

² Met Office Hadley Centre, FitzRoy Road, Exeter EX1 3PB, UK

Segele et al. 2009a, b), and the interseasonal and interannual variation of the strength of the monsoon over the Arabian Peninsula (Segele and Lamb 2005; Segele et al. 2009a, b). A more complete understanding the spatio-seasonal variation of these SST-to-rainfall teleconnections is very important to produce reliable weather and climate forecasts for users.

The spatial and temporal distribution of climatological rainfall in Ethiopia is largely controlled by the annual north–south migration of the Inter Tropical Convergence Zone (ITCZ) (Kassahun 1987) over Ethiopia’s complex topography. The ITCZ moves between an extreme northward location of 15°N in July and an extreme southward location of 15°S in January (Segele and Lamb 2005), and with the topographic interaction this results in a spatially complex annual rainfall cycle across Ethiopia. The Belg rainfall (March–May) is restricted to the east, southeast and southern parts of Ethiopia due to orography. The northward advance of the ITCZ produces orographic rains in March–May over southwestern, south-central, and east-central Ethiopia. Low pressure over South Sudan draws in a moist flow from the Indian Ocean and Gulf of Aden (Segele et al. 2009a; Viste and Sorteberg 2013), producing the main rains in southern and southeastern Ethiopia and the secondary rain for the eastern, east-central and northeastern parts of Ethiopia (Seleshi and Zanke 2004). Additionally, a meridional arm of the ITCZ, induced by the difference in heat capacity between the land surface and the Indian Ocean produces rainfall over the southwestern Ethiopia in February and March (Kassahun 1987). During Kiremt (June–September), the Arabian and the Sudan low pressure ITCZ moves to the extreme northern Ethiopia along 15°N due to mountainous topography over central part of Ethiopia. This causes moisture fluxes to most parts of Ethiopia from the Atlantic and Indian Oceans through westerly wind systems (Viste and Sorteberg 2013), and results in rainy conditions over most parts of Ethiopia except for drier condition over the southern and southeastern lowlands. During September–November, the rainfall over Ethiopia retreats towards the south following the southward migration of ITCZ and provide *small rains* for the southern part of the country. During Belg (December–February), the ITCZ is located well south of Ethiopia and the country predominantly falls under the influence of dry warm and cool northeasterly winds. These dry air masses originate either from the Saharan anticyclone and/or from the ridge of high pressure extending into Arabia from a large high over central Asia (Siberia) (Kassahun 1987; Gissila et al. 2004). Therefore, based on the climatological annual cycle, Ethiopia has previously been divided into three major subregions; the northern and central-western part of the country has a single rainy season with a peak in July/August, central and eastern Ethiopia has two rainy

periods February/March–May (Belg) and June–September (Kiremt), and southern Ethiopia has two rainy seasons, the Long Rains (March–May) and the Short Rains (September–November) (Diro et al. 2011b).

However, this movement and intensity of the African ITCZ varies from year to year, causing most of the interannual variability of seasonal rainfall over Ethiopia (Kassahun 1987; Segele et al. 2009a). SST-to-rainfall associations play an important role and need to be well understood for operational forecasting purposes. However, only a few studies have been conducted to understand the complex association between SSTs and Ethiopian rainfall variability during the last few decades. Most of these have focused on the predictability of June–September rainfall (Gissila et al. 2004; Korecha and Barnston 2007; Diro et al. 2011a). These and other related studies, such as Segele et al. (2009a, b); and Diro et al. (2011a) suggest that the interannual rainfall variability during this season is ultimately controlled by large-scale SST anomalies over the equatorial east Pacific (the El Niño–Southern Oscillation; ENSO) and the Indian Ocean, where warming/cooling events are associated with deficit/excess of rainfall over the central and northern half of the country. A few of these studies, such as Segele and Lamb (2005); Segele et al. (2009a, b); and Diro et al. (2011a) also reported the presence of some correlation between SSTs over the southern Atlantic Ocean and Gulf of Guinea and Ethiopian June–September rainfall.

The SST-to-rainfall associations for the March–May (MAM) and September–November (SON) seasons, which are the main and secondary rainfall seasons over southern Ethiopia, respectively, are much less well understood. Only Diro et al. (2008) has used the SST anomalies from the Atlantic, Indian and Pacific Oceans to predict the MAM rainfall. Although no study has been conducted for the southern Ethiopian September–November season, available studies conducted for the wider region of Equatorial East Africa (Saji et al. 1999; Behera and Yamagata 2003; Black et al. 2003; Marchant et al. 2006; Saji and Yamagata 2003) show that anomalous warming (cooling) over the equatorial East Pacific and Indian Ocean are associated with enhanced (suppressed) rainfall amounts in this wider region. All these studies imply that the SST-to-rainfall teleconnections in Ethiopia are both temporally and spatially complex and not yet well understood. Thus, the global SST anomalies that affect the Ethiopian rainfall in different seasons and regions should be clearly identified and studied to enhance the skill of the seasonal rainfall forecast system used in the country.

Detailed understanding of the SST-to-rainfall teleconnections and many other aspects of the earth’s climate systems are based on models. In this regard, global circulation models (GCMs) are critical tools that aid our understanding

of the complex global atmospheric circulation and also enhance weather and climate prediction skill (Collins et al. 2011). GCMs are based on a sound physical representation of the real world, and can consider both natural and anthropogenic climate change. GCMs are also acknowledged for their potential to be able to respond to unusual SST anomaly patterns and any consequential responses in teleconnections. Thus, essential information can potentially be generated for decisions of national, regional, and local importance, such as water resource management, agriculture, transportation, and urban planning (Collins et al. 2011; Martin et al. 2011). Currently, the demand for climate model data is growing due to this increasing interest in climate information (Hewitt et al. 2011). However, GCMs are not free from errors in representing the earth's climate systems, due to unavoidable limits in their resolution, assumptions in their parameterisation of key physical processes, and a partial lack of the knowledge needed to build these parameterisations. Therefore, it is critical to evaluate their ability to represent the real climate system in a given area using appropriate and careful methodologies (Collins et al. 2011). Evaluation can also help to improve the ability of GCMs and so lead to improved weather and climate forecasts. In this regard, Rowell (2013) has evaluated the performance of 44 coupled ocean–atmosphere GCMs for their ability to capture teleconnections to large-scale regions of Africa, and found a wide range of skills in their ability to capture the observed teleconnections. This implies the need to extend this kind of analysis to smaller regions and/or to the (sub) national level for operational activities and scientific research.

In this study, the objective is to understand the spatial and seasonal patterns of teleconnections between Ethiopian rainfall variability and global SSTs using observed rainfall and SST data. Hence, this study provides a comprehensive view on the general patterns of the SST-to-rainfall teleconnections across both time and space for Ethiopia. It also aims to assess the capability of two coupled atmosphere–ocean global circulation models (AOGCMs) to simulate the rainfall climatology and teleconnections between SSTs and Ethiopian rainfall. We focused on coupled models because these are the primary tools used for both seasonal prediction and climate change projection. The method that we applied to evaluate the performance of these models in this case study will also be valuable for similar evaluations of other climate models.

2 Data and methods

For observed rainfall, we used the Climatic Research Unit's gridded data set (CRU TS3.1) described by Harris et al. (2014). This dataset provides monthly mean precipitation totals at 0.5° spatial resolution for the period 1901 to

the present day. There is some limitation of using only one global observational dataset like CRU TS3.1 due to some inherent uncertainties such as low density of reference gauging stations considered for reanalysis in some areas (such as Sub-Saharan Africa) and the presence of missing data for some years (Harris et al. 2014). However, Dinku et al. (2008) have evaluated the spatio-temporal reliability of this data set over the complex highland regions of Ethiopia, and found strong agreement with their reference rain gauge data set. Similarly, Tsidu (2012) evaluated the spatio-temporal reliability of CRU and other gridded data sets using rainfall records of 233 gauge stations over Ethiopia for the 1978–2007, and found statistically significant correlations of 0.81–0.95 over central and northern Ethiopia, 0.66–0.80 over western and southeastern Ethiopia, and 0.52–0.65 over other parts of the country. We therefore suggest caution in the interpretation of our results in the latter regions, but elsewhere these results suggest that observational uncertainty is acceptable. The CRU monthly rainfall data set has also been used for more detailed teleconnection analysis over Upper Blue Nile Region (Zaroug et al. 2014a, b). For our study, we considered the rainfall data for the period 1955–1995 to maintain the quality of data because in the early twentieth century some stations had not been established, and from the end of the twentieth century some stations had ceased reporting or their data was not readily available. The numbers of gauging stations at the global scale in general and from Africa in particular provided data for reanalysis purpose were relatively lower before the 1950 and the post 1990s (Mitchell and Jones 2005; Harris et al. 2014). Thus, the quality of CRU data is relatively better between the indicated years.

Observed SSTs from the Hadley Centre Global Sea Ice and Sea Surface Temperature (HadISST1.1) data set at 1° × 1° resolution, described by Rayner et al. (2003), were used. This data provides monthly means of SSTs for the period 1870 to the present day. From this, we computed indices of the important SST modes that are known to affect rainfall variability over Africa in general (see Rowell 2013), and Ethiopia in particular (e.g. Segele et al. 2009a, b; Diro et al. 2011a). Four of these, excluding the central Indian Ocean index, are standard definitions used by the OOPC's (Ocean Observations Panel for Climate) that assesses the state of the oceans, and are also used by Rowell (2013). The SSTs indices considered over the Indian Ocean are the central Indian Ocean index (CIndO) average over (55°E–95°E and 25°S–10°N) as described in Rowell (2013), and the Indian Ocean Dipole (IOD) which is the average over (10°S–10°N and 50°E–70°E) minus the average over (10°S–0 and 90°E–110°E) as described in Saji et al. (1999). Over the Pacific, we use the Niño3.4/ENSO average over (170°W–120°W and 5°S–5°N) that is

largely used for seasonal rainfall forecasts for the June–September season in Ethiopia (Korecha and Barnston 2007). Over the Atlantic Ocean, we use the tropical Atlantic Dipole (TAD) that is the difference between a tropical North Atlantic average (5°N–25°N and 15°W–55°W) minus a tropical South Atlantic average (0°–20°S and 10°W–30°W) as described in Enfield et al. (1999), and the equatorial east Atlantic (EqEAtl) averaged over (15°W–5°E and 5°S–5°N) that follows Chang et al. (1997).

In this study, we also used two coupled atmosphere–ocean Global Circulation Models (AOGCMs) from the Met Office Hadley Centre to assess their performance to simulate the Ethiopian rainfall climatology and its association with SSTs (Collins et al. 2011; Hewitt et al. 2011; Martin et al. 2011). These models are: HadGEM2 (Hadley Centre Global Environment Model version 2) with a spatial resolution of N96 (1.25° latitude by 1.875° longitude) described in Collins et al. (2011); and Martin et al. (2011); and two resolutions of HadGEM3-GA3.0 (Hadley Centre Global Environment Model version 3 with Global Atmosphere version 3.0) as described in Hewitt et al. (2011). The two spatial resolutions of HadGEM3-GA3.0 are N96 (1.25° latitude by 1.875° longitude) and N216 (0.555° latitude by 0.833° longitude). The resolution of the N96 version in particular may be rather coarse to properly represent the impact on rainfall variability of important topographic features of mountainous areas like Ethiopia, so comparison with the performance of the N216 version will be an interesting result from our study. We also note that HadGEM3-GA3.0 is a climate model that was under continuous improvement (Hewitt et al. 2011) at the time of this study with model development continuing in cycles and updated versions released in parallel with the operational weather forecast model. Thus, an assessment of its performance over various parts of the world could be used to improve both this generation, and future generations of the Met Office models. Last, we note that no forcings, natural or anthropogenic, were used to drive our chosen model experiments, and so they provide ‘control’ data for an undated period that is consistent with the current climate.

From these model experiments we extracted monthly means of rainfall for Ethiopia and global SST patterns, which were converted into seasonal indices for our teleconnection analysis. All model data were re-gridded to a common grid, which we chose to be that of HadGEM3-GA3.0-N216. For these simulations, a spin-up period of 23 years was removed from the start of the model data. The remaining length of time considered for our analysis is 74 years for HadGEM2-N96 and HadGEM3-GA3.0-N96, and 59 years for HadGEM3-GA3.0-N216.

3 Seasonal cycle of observed teleconnection patterns over Ethiopia

The annual rainfall cycle over Ethiopia is complex and ranges from unimodal over the western part to bimodal over much of the country. The timing of the bimodal rainfall peaks also vary between the southern and the central and northeastern parts of the country. Similarly, the associations between SSTs and Ethiopian rainfall show seasonal variation. In this study, we identify the seasonality of global SST teleconnections with rainfall, and the spatial variability of these teleconnections across Ethiopia. The data period used for this purpose was 41 years (1955–1995). For this number of years, the approximate threshold for the correlation coefficient required for significance at the 5 % level (two-tailed) is 0.30.

3.1 Definition of the rainfall seasons

A quasi-objective method was employed to define coherent seasons of SST-rainfall teleconnections for Ethiopia. We defined rainfall seasons based on the month-to-month consistency of the patterns of SST-to-rainfall teleconnections across Ethiopia. To do so, five SSTs time series (TAD, EqEAtl, CIndO, IOD and Niño3.4) that are known to affect the Ethiopian rainfall (Gissila et al. 2004; Korecha and Barnston 2007; Diro et al. 2011a) were correlated against the gridded Ethiopian rainfall, CRU TS3.1 (0.5° × 0.5°). Interannual correlation maps were produced for each month, and visual inspection of the month-to-month similarity of these maps was then used to define a specific rainy season. Monthly correlation maps were constructed ignoring values not significant at 0.5 level. Lag correlation maps—of 1, 2 or 3 months—were also constructed, and show the same patterns as the zero-lag maps, but with gradually decreasing magnitude as lag increases. Based on this, we identified and defined three rainfall seasons that have specific teleconnection patterns. These are March–May, July–September and October–November (Fig. 1). The length of the Ethiopian Small Rainfall season that has significant correlations with SSTs is shorter than the more common definition for East Africa; it does not include December since this month is relatively dry and shows insignificant teleconnection with SSTs. Here, the definitions of Ethiopian rainfall seasons for Kiremt (over most part of the country except southern Ethiopia) and the small rainfall season (over southern Ethiopia) vary a little bit from what the Ethiopian National Meteorological Agency (NMA) recognizes with the omission here of June and September, respectively. This is because we focus here

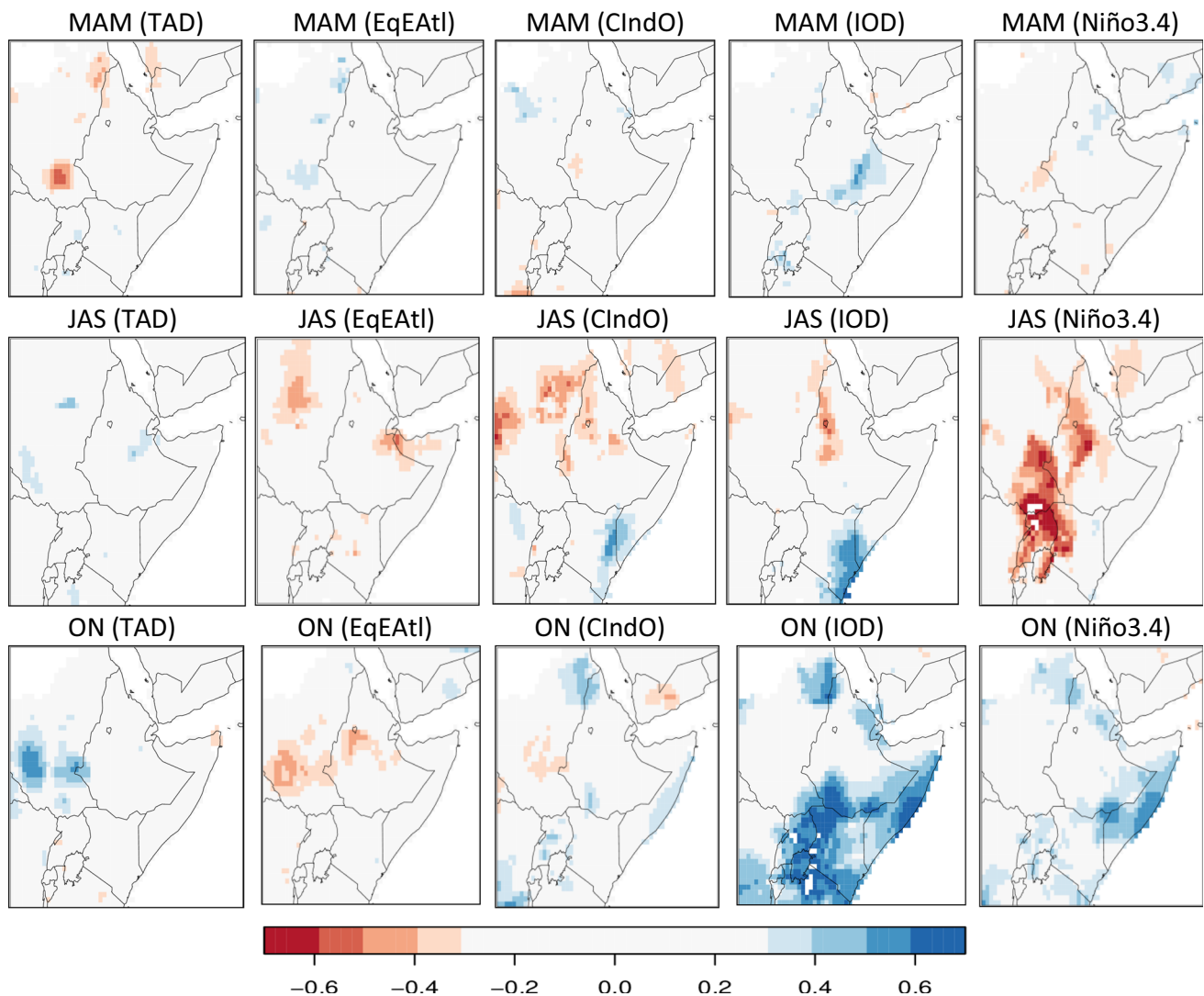


Fig. 1 Correlation of five observed SST indices (shown above each panel) with observed seasonal gridded rainfall over Ethiopia for the period 1955–1995. SST and rainfall data are averaged over the season

shown above each panel. Correlation magnitudes of 0.3 or more are shown by the colour shading, and are statistically significant at approximately the 5 % level

on consistency of rainfall–SSTs correlations for the benefit of seasonal prediction, rather than on climatological rainfall totals. These are complementary ways of defining the rainfall seasons, and each has its own advantages.

3.2 Spatial variability of the seasonal teleconnections over Ethiopia

Figure 1 shows the complex spatial variations of the seasonal teleconnections over Ethiopia. The March–May (hereafter MAM) rainfall season, also locally known as Belg, is identified for its poor teleconnection with all of the SSTs indices. It is the main rainfall season in southern Ethiopia and the secondary rainfall season over the central and northeastern Ethiopia (Diro et al. 2008), but its

teleconnections with global SSTs are weak and statistically insignificant. Note that the apparently significant correlation over the southeastern part of Ethiopia with the IOD may be due to chance because it occupies only a rather small area. Similarly, previous studies (Hastenrath et al. 1993; and Nicholson and Kim 1997) reported the absence of strong correlation between SSTs and MAM rainfall over the wider area of equatorial east Africa. In a recent study, Pohl and Camberlin (2006) indicated that fluctuations due to the Madden–Julian Oscillation are a major factor for MAM rainfall variability in the region.

For July–September (hereafter JAS), which is the main rainfall season over most parts of the country, also locally known as Kiremt, we found strong and statistically significant rainfall negative correlations with Niño3.4, the

IOD and CIndO SSTs. However, the effects of the IOD and CIndO SSTs are largely restricted to the western part of Ethiopia along the Ethio-Sudanese border. Segele et al. (2009a, b); Diro et al. (2011a) report similar results, and Diro et al. (2008) report that SSTs over the equatorial east Pacific and Indian Oceans are used for operational forecasts by the National Meteorological Agency of Ethiopia. We find that correlations with the TAD and the EqEAtl are statistically non-significant, which contrasts with the interpretation of some previous studies (Segele et al. 2009a, b; Diro et al. 2011a) and requires further examination.

The October–November (hereafter ON) period is also known as the Small Rains, except usually with the inclusion of September in southern Ethiopia (Degefu and Bewket 2014) or the inclusion of December elsewhere in equatorial east Africa (Black et al. 2003). We find that rainfall variations during October and November show similar statistically significant patterns of positive correlation between the IOD (or Niño3.4) and gridded rainfall over Ethiopia. In contrast, the pattern of correlations for September is quite different, and that for December is statistically insignificant. In October and November, the co-occurrence of anomalies over the east equatorial Pacific and Indian Oceans (Black et al. 2003), and the Zonal Dipole Mode over the Indian Ocean (IOD) (Saji et al. 1999; Behera and Yamagata 2003; Saji and Yamagata 2003; Marchant et al. 2006) are known to affect the equatorial east African Short rains, and here we show there are also significant correlations with southern Ethiopia. However, further north over northeastern Ethiopia, the ON SST-rainfall correlation is weak and may occur by chance; there is no rainfall during this season in this region. Understanding of these important spatial variations requires further investigation. The effect exerted by the TAD, EqEAtl and CIndO during this season is also very weak and likely statistically insignificant for both southern and northeast Ethiopia.

3.3 Regionalisation of teleconnection patterns over Ethiopia

As shown in Sect. 3.2, the SST-to-rainfall teleconnections for Ethiopia not only vary seasonally, but also spatially. Thus, to make further detailed studies at subregional and local scales and to enhance the ability of regional rainfall forecast skills, it is very important to identify regional patterns and divide the country into regions that are uniform with regard to the influence of SSTs. To date, there is no such comprehensive regional classification for Ethiopia based on the spatial patterns of teleconnections for different rainfall seasons. The regional classifications by previous studies (e.g. Gissila et al. 2004; Diro et al. 2011a, b)

were only for one rainfall season (JJAS), and not based on the spatial variation of teleconnections, but rather were based on the homogeneity of rain gauge stations for their annual cycles and interannual correlations of seasonal rainfall amounts. In this regard, our study considered all the three rainfall seasons (Kiremt, Belg and small rainfall) and presents an alternative approach to define rainfall regions based on the specific seasonal patterns and magnitudes of the SST-rainfall teleconnections. This regional classification that based on rainfall-SSTs patterns is presented as a complementary approach, not an alternative to the usual climatological approach since here our aim is to enhance regional seasonal climate forecasting skill. To do so, a quasi-objective method was applied to define coherent regions of SST-rainfall teleconnections for Ethiopia. Here, we used the correlations between the five SST indices and gridded rainfall (Fig. 1). Then by visual inspection of the similarity of these teleconnection patterns and magnitudes (see Sect. 3.1), we identified three broader teleconnected rainfall regions (Fig. 2).

The first region is central and western Ethiopia (hereafter CW-Ethiopia) for which JAS is the main rainfall season and shows statistically significant negative correlations with Niño3.4, CIndO and the IOD. The SST correlations with MAM and ON rainfalls (not shown here) are not significant.

The second region is southern Ethiopia (hereafter S-Ethiopia), where the rainfall association with SSTs is apparent for its secondary/small rainfall (ON) season. The rainfall over this region is positively related with Niño3.4 and IOD, and is statistically significant. No correlation was found for the MAM and JAS seasons. Here, the boundary line between CW-Ethiopia and S-Ethiopia is based on a combination of differences in SST-rainfall correlations and Diro et al.'s (2008) climatological rainfall zones.



Fig. 2 Definition of the rainfall regions based on their teleconnection patterns, and used to average rainfall

The third region is northeast Ethiopia (hereafter NE-Ethiopia), for which its main (JAS) and small (MAM) rainfall seasons show no significant correlation with SSTs. The ON season appears to show significant positive correlation with Niño3.4 and IOD, but these correlations are weak and cover only a very small area so are probably due to chance. Also, this region is known for its dry climate during this season.

3.4 Teleconnections from SSTs to regional average rainfall

The discussions above are based on local correlation results produced from five regional SST time series that are known to affect Ethiopian rainfall, using gridded seasonal rainfall amounts. Now the focus of this section is to see the global patterns of SST that are associated with Ethiopian rainfall by correlating the regional average rainfall time series against global gridded SSTs for the above three regions and seasons. Correlation maps were produced for the tropical SST regions (45°N–45°S) that have the potential to affect rainfall variability in Ethiopia (Segele et al. 2009b). As shown in Sects. 3.2 and 3.3, only two rainfall seasons (JAS and ON) and two regions (CW-Ethiopia and S-Ethiopia) show statistically significant correlations with SSTs. This section focuses on these two seasons and regions.

Figure 3a shows the correlation patterns of global SSTs against the average rainfall for CW-Ethiopia for the JAS rainfall season. As we described in Sects. 3.2 and 3.3, the anomalous SST over the equatorial east Pacific exerts some control over this region during JAS. It is evident that the occurrence of drought and excessive rainfall over this region is somewhat associated with warm (El Niño) and cold (La Niña) events, respectively. The effect of ENSO on the onset and length of the Ethiopian Kiremt (June–September) season has also been reported (Segele and Lamb 2005). The physical mechanisms of these relationships are presented in previous studies (Segele and Lamb

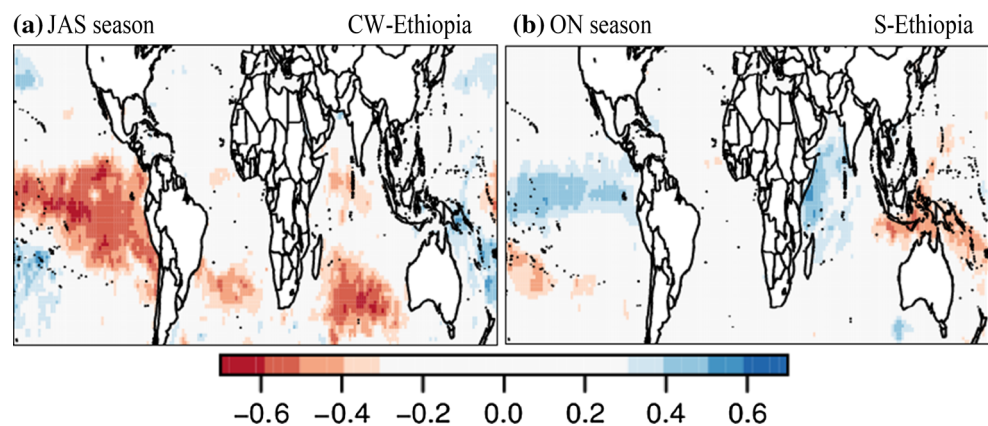
2005; Segele et al. 2009a, b; Diro et al. 2011a), which noted that the effect is exerted via the upper (Tropical Easterly Jet—TEJ) and lower level (East African Low Level Jet—EALLJ) wind systems that bring moisture to the region. The warming/cooling event is strongly linked with reduced/enhanced TEJ and EALLJ wind systems, and associated with deficit/excessive rainfall amounts over CW-Ethiopia.

Similarly, the SST over southern Indian Ocean shows some significant and negative correlation with the CW-Ethiopia JAS rainfall. As it was mentioned in Gissila et al. (2004) and Segele et al. (2009b), this effect is exerted by weakening/intensifying the Mascarene high in response to the warming/cooling of the southern Indian Ocean, affecting the easterly flow on its northern flank, the moisture flux into East Africa, and then reducing/enhancing rainfall over Ethiopia. The findings of our study, therefore, support this view.

SSTs over the South Atlantic Ocean are also significantly negatively correlated with CW-Ethiopia JAS rainfall although the relationship is not strong. This result generally supports the findings reported by Segele et al. (2009b), but does not agree with Diro et al. (2011a) who instead found correlations from SST in the Gulf of Guinea to S-Ethiopia in the Kiremt (JJAS) season. Reasons for this discrepancy are unclear. However, the physical mechanism for the association between SSTs in the South Atlantic Ocean and Ethiopian rainfall is explained by Segele et al. (2009b). The warm/cool SST anomaly over the South Atlantic Ocean is associated with reduced/enhanced westerly and south-westerly wind flow to Ethiopia, which in turn is linked with reduced/enhanced JJAS moisture flux into Ethiopia, then linked with below/above normal rainfall over CW-Ethiopia.

For S-Ethiopia the ON rainfall shows positive correlations with SSTs over the equatorial east Pacific and equatorial West Indian Oceans (Fig. 3b). This is an important finding of this study since the Ethiopian ON rainfall season

Fig. 3 Correlation of observed rainfall, averaged over **a** CW-Ethiopia and **b** S-Ethiopia with observed SSTs for the period 1955–1995. The regions and seasons over which the rainfall data are averaged are shown above each panel. Correlation magnitudes of 0.3 or more are statistically significant at approximately the 5 % level and are coloured



has not been given emphasis in previous studies. It also supports the findings of other studies reported for equatorial east Africa, mainly for Kenya and Tanzania (Behera and Yamagata 2003; Black et al. 2003; Marchant et al. 2006; Ummenhofer et al. 2009). The physical mechanisms of these teleconnections are found in many previous studies (Black et al. 2003; Saji and Yamagata 2003; Marchant et al. 2006; Ummenhofer et al. 2009). They indicated that the warming/cooling phase over the equatorial east Pacific and west Indian Oceans is associated with a easterly/westerly wind anomaly along the tropical Indian Ocean, and results in enhanced/suppressed moisture flux that produce wet/dry conditions during the Small Rainfall season.

The interannual rainfall variability in JAS for CW-Ethiopia and ON for S-Ethiopia, and the associated modes of SST (Niño3.4 and IOD), are shown in Fig. 4. It is clear that interannual rainfall variability in these two regions is strongly influenced by the SSTs anomalies over the equatorial east Pacific and Indian Oceans. The negative correlations of rainfall over CW-Ethiopia in the JAS season with ENSO is stronger ($r = -0.59$) than with the IOD ($r = -0.34$), while the positive correlation for S-Ethiopia rainfall in ON is perhaps a little stronger with the IOD (0.56) than with ENSO (0.45).

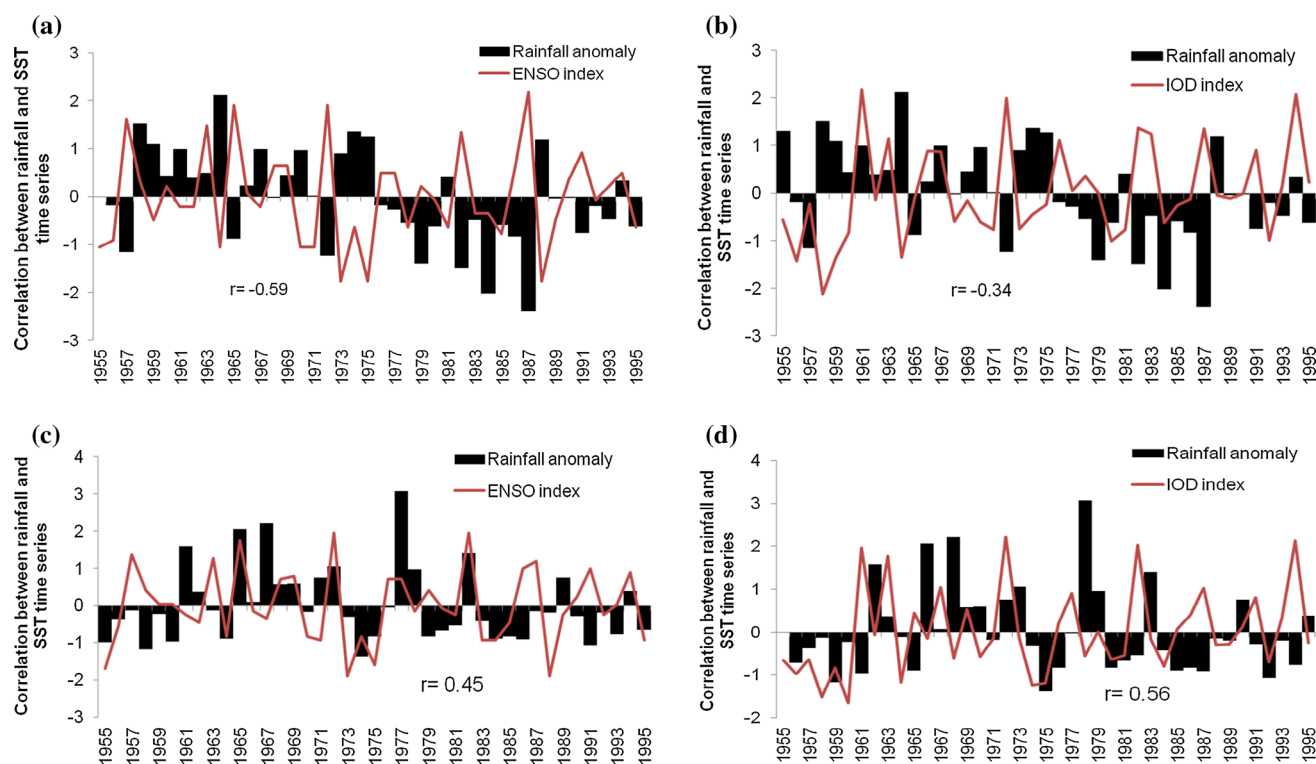


Fig. 4 Time series of standardised seasonal rainfall variability and Niño3.4 and IOD indexes for the period 1955–1995; **a** and **b** present the association between the JAS rainfall variability in the CW-Ethiopia with ENSO and IOD indexes, and **c** and **d** present the

4 Model evaluation for representing the rainfall climatology and teleconnection

The main objective of this section is to evaluate the performance of HadGEM2 and HadGEM3-GA3.0 in representing Ethiopian rainfall variability and its teleconnections with global SSTs. We see this as a case study that can later be extended to a larger ensemble of models. Section 4.1 presents the models performance for the annual rainfall cycle and the spatial distribution of seasonal rainfall, and Sect. 4.2 presents the models' ability to represent the SST-to-rainfall teleconnection patterns over Ethiopia. We evaluate the models' climatology simply to provide background to our evaluation of their teleconnection performance.

4.1 The models' ability to represent annual cycles and spatial patterns of seasonal rainfall

Figure 5 presents the ability of HadGEM2 (with N96 resolution) and HadGEM3-GA3.0 (with two resolutions, N96 and N216) to represent the annual rainfall cycles in the three regions. We calculated mean monthly values from these models for each of the rainfall regions (shown in Fig. 2), and compared that against the observations (CRU

association between the ON rainfall variability with Niño3.4 and IOD indexes. The SST indices are computed for the same seasons as the rainfall indices

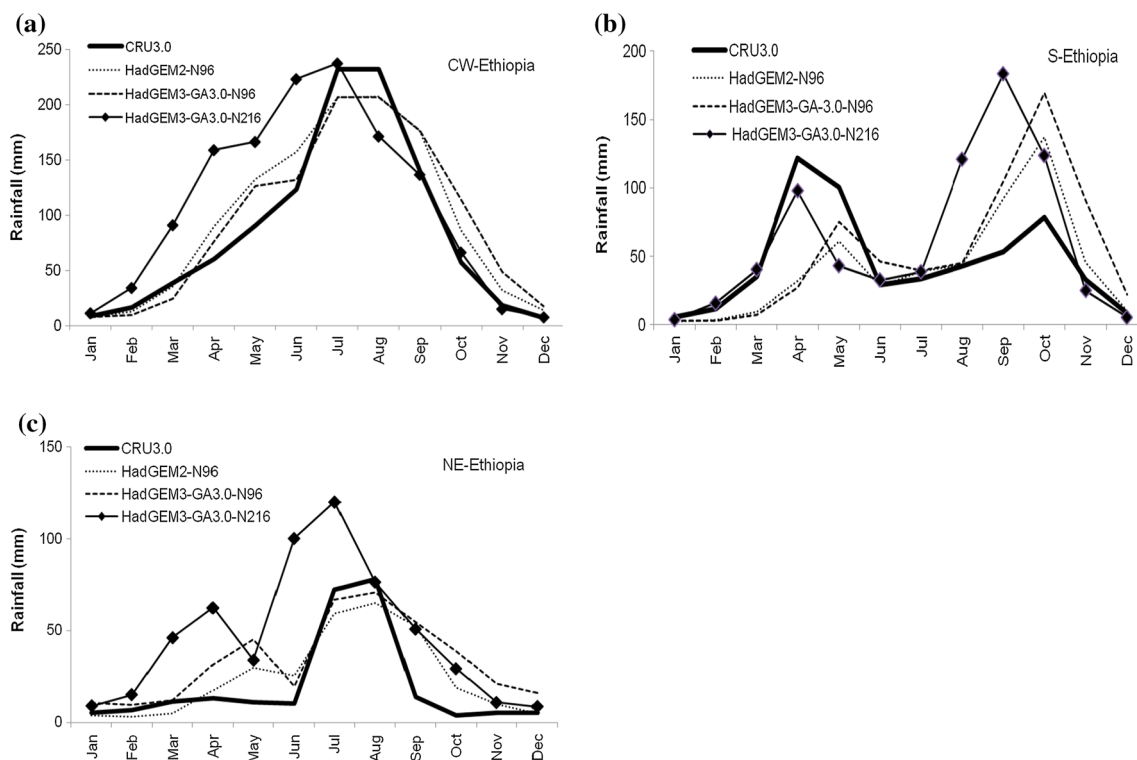


Fig. 5 Observed and modelled annual cycle of rainfall over **a** CW-Ethiopia **b** S-Ethiopia and **c** NE-Ethiopia. Observed (CRU3.0) data are for the period 1922–1995. Model data are 74-year means for

HadGEM2-N96 and HadGEM3-GA3.0-N96, and 59-year means for HadGEM3-GA3.0-N216 simulations

TS3.0). It can be seen in Fig. 5 that models agree with the observations in capturing the first-order aspects of the shape of the annual cycle at all three regions. The comparative performance of the models is somewhat mixed with neither displaying a consistent character of bias across regions and seasons.

Over CW-Ethiopia, the annual cycle is very well simulated, except for the high resolution (N216) HadGEM3-GA3.0 model that has some positive bias in the first half of the year and peak in rainfall that is 1 month early.

Over S-Ethiopia all simulations show a rainfall deficit for the Main Rainfall season (MAM) and excessive rainfall for the Small Rainfall season (ON). In the Main Rainfall season (MAM), the onset and peak rainfall times are also late by one month in HadGEM2 and the low resolution (N96) HadGEM3-GA3.0, whereas the high resolution (N216) version of HadGEM3-GA3.0 has less bias and an April peak as observed. In the Small Rains (ON), the high resolution (N216) HadGEM3-GA3.0 model has a too early start and peak date.

Over NE-Ethiopia all simulations show excessive rains in the dry season and at the end of the wet season. In addition to this, the high resolution (N216) HadGEM3-GA3.0 model has an early start and excessive rain before the wet season.

Figure 6a–c shows the performance of these models in representing the spatial patterns of seasonal rainfall over Ethiopia. The left-hand panels show the observed mean rainfall (CRU3.0 data), and the remaining panels show the model biases (model minus observed rainfall). Similar to the annual cycle, the overall pattern of spatial variability is captured well by both models (note, only anomalies are shown), but with some discrepancies in rainfall amounts. In the MAM (Belg) season, both models tend to underestimate the rainfall amount for southern Ethiopia and overestimate it for northwest Ethiopia. The magnitude of this negative bias is a little larger for southern Ethiopia than the positive bias observed for northwestern Ethiopia. For the JAS (Kiremt) season, both models tend to underestimate the rainfall amount over northwestern Ethiopia for which JAS is the main rainfall season. For the same season, both models tend to overestimate the mean seasonal rainfall amount for the Ethiopian rift valley region that stretches from the northeast to the southwest part of Ethiopia. Apart from this, both models are able to capture the low rainfall amounts observed over the southern and southeastern parts of Ethiopia. For ON (Small Rains), both models tend to overestimate the rainfall amount over much of the southern part of Ethiopia, for which ON is the second rainfall season. Compared with HadGEM2, the HadGEM3-GA3.0

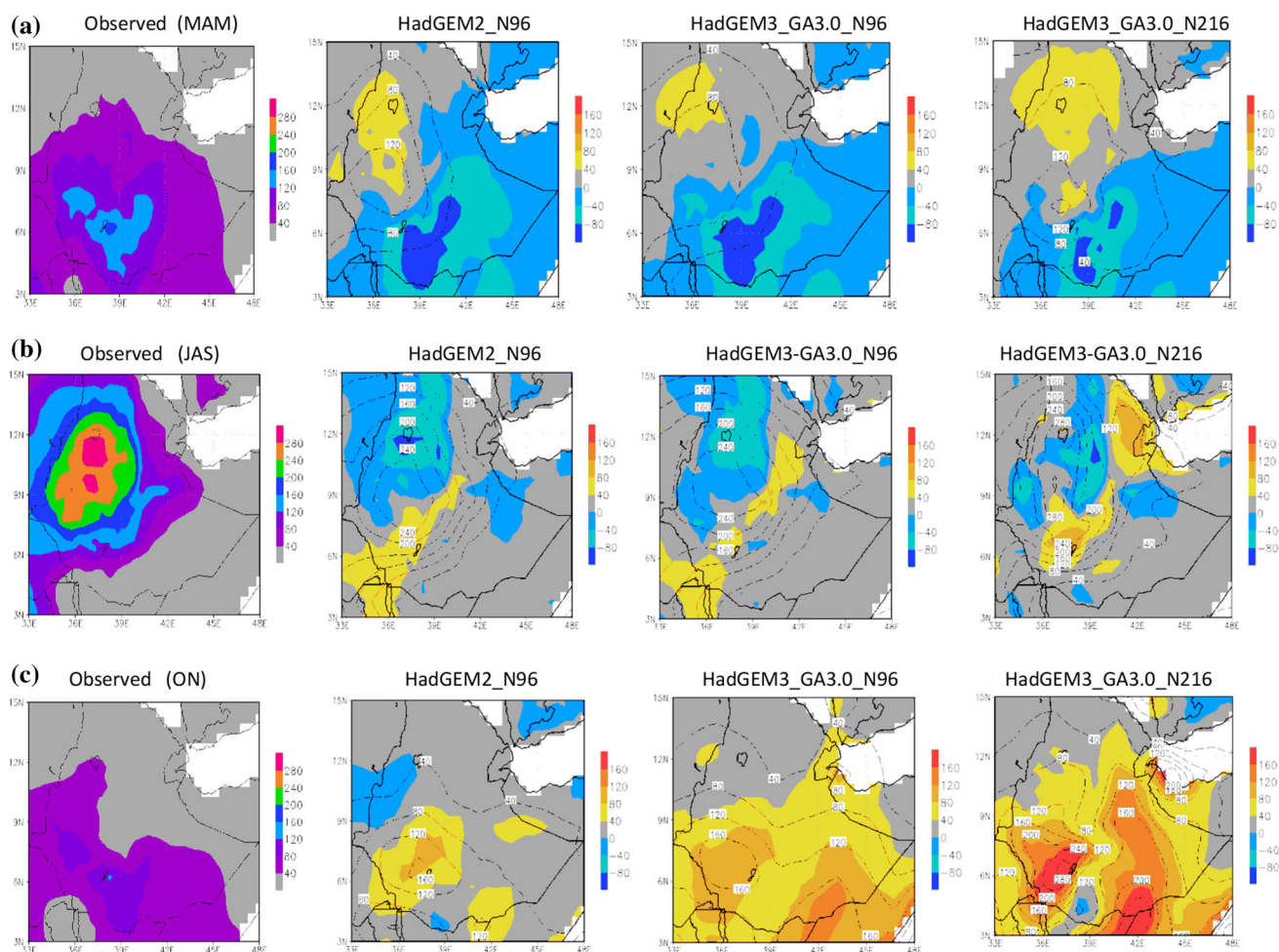


Fig. 6 Comparisons of model rainfall biases for **a** MAM, **b** JAS, and **c** ON seasons over Ethiopia for the period 1955–1995, with contours showing each model’s seasonal total for that season. The *left-hand*

column shows the observed seasonal totals (CRU3.0) for reference. (Rain amount is presented in mm)

model greatly overestimates the rainfall over two distinct regions aligned north–south cover much of southern and eastern Ethiopia. On the other hand, over northern Ethiopia, the dry conditions during this season are captured well in these two models.

Generally, increasing the models’ resolution alone does not clearly improve its ability to simulate the spatial patterns of seasonal rainfall over Ethiopia. This may be because a ‘threshold resolution’ has not been crossed, which might improve the regional climatology either by resolving important orographic features or by improving the scale interactions of relevant local dynamics or remote dynamics such as air–sea coupling and teleconnections. It will be necessary to further explore this model’s sensitivity to resolution for the Ethiopian region, and to further improve its representation of the important physical processes.

4.2 Model ability to represent SST-to-rainfall teleconnection patterns over Ethiopia

Figure 7 shows the performance of HadGEM2 and HadGEM3-GA3.0 for their ability to simulate some of the seasonal and spatial variability of SST-rainfall teleconnections over Ethiopia (see Collins et al. 2011; Hewitt et al. 2011; and Martin et al. 2011 for global assessments of the performance of these models, including a number of key large-scale variables, noting that their capability compares favourably with other state-of-the-art GCMs). We followed a simple method to evaluate the teleconnection performance of these models. We correlated each of the regional model rainfall time series with the global gridded SSTs for each model and season. Then, these correlation maps were visually compared against the observed teleconnection plots shown in Fig. 3a, b (and also with those not shown).

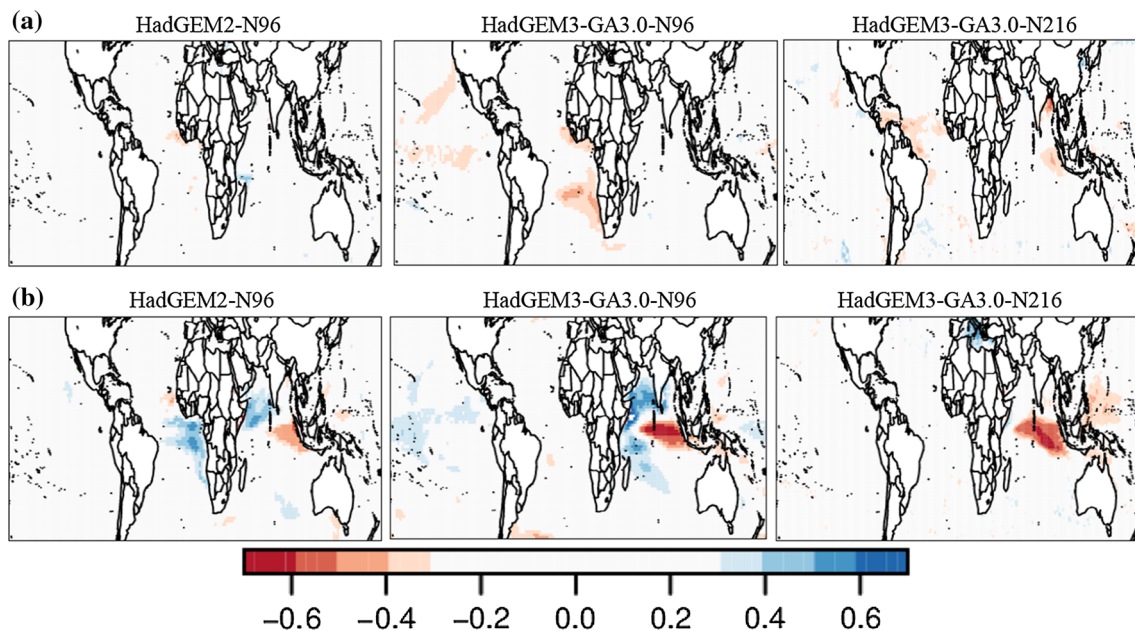


Fig. 7 Comparisons of coupled atmosphere–ocean model runs with observed climate data for the SST-to-rainfall teleconnections for Ethiopia, for the **a** JAS rainfall season over CW-Ethiopia and **b** ON

season over S-Ethiopia. Correlation magnitudes of 0.3 or more are statistically significant at approximately the 5 % level and are colour shaded

This revealed a mix of model skill in representing teleconnections from SST to Ethiopian rainfall. The model teleconnection plots presented here are only those for JAS for CW-Ethiopia and ON for S-Ethiopia, where the observed rainfall data show statistically significant correlations with SSTs.

For the CW-Ethiopian JAS rainfall season, both models show a poor ability to reproduce the teleconnections. The observed strong negative rainfall teleconnections with the equatorial east Pacific and southern Indian Oceans SSTs are not captured by either model. Only the low resolution version of HadGEM3-GA3.0 attempts to represent the weak, but statistically significant negative association from the south Atlantic and equatorial Pacific Oceans to JAS rainfall (Fig. 7a).

For the S-Ethiopian ON rainfall season, the models show a mix of skills. Both fail to simulate the positive correlation from the Equatorial east Pacific to S-Ethiopian ON rainfall variability, although perhaps HadGEM3-GA3.0 (N96) very weakly captures it. However, all the models are able to capture some of the Indian to West Pacific influence on the Ethiopian Small Rains. HadGEM2 and the low resolution (N96) HadGEM3-GA3.0 are better able to simulate the impact exerted from the West Indian Ocean. On the other hand, over the tropical Atlantic Ocean (Gulf of Guinea), the positive SST association with ON Rainfall that is simulated by HadGEM2 is nonexistent in the observations (Fig. 3b).

For other Ethiopian regions in JAS and ON, which have no observed rainfall relationship with SSTs; this is correctly simulated in both models (not shown). Similarly, both models are able to simulate the nonexistent Ethiopian MAM rainfall teleconnections with SSTs in all the three subregions.

Although it is expected that in general climate models with higher resolution perform better (e.g. Roberts et al. 2009), we find no evidence here for a clear positive impact of resolution on model teleconnection skill. Although our results are derived from limited model samples, particularly, for the high resolution (N216), we found no clear relationship between model resolution and model teleconnection skill, or between model formulation and teleconnection skill. Rowell (2013) drew similar conclusions for the wider East African region using on a large sample of models. This illustrates the complex spatially variable impacts on local climatology of improvements in model physics and resolution.

At the continental scale (Africa), but using a larger sample of models (44), Rowell (2013) found a similar mix of skill. He also found HadGEM2 is amongst the better models, so we suggest it is likely that the HadGEM2 and HadGEM3-GA3.0 performance shown here in representing teleconnections to Ethiopia is probably no worse than many other models. However, a comparison with Rowell's results shows the mixed skill found here for the Small Rains in subregions of Ethiopia is inferior to the “at least

reasonable skill” found for the much larger Greater Horn of Africa (GHA) region. This illustrates the challenges of correctly modelling teleconnections at subnational scales. (Note that Rowell did not analyse MAM and JAS teleconnections to GHA.) Rowell (2013) also suggested that errors in coupled model teleconnections may primarily arise from errors in the coupled models’ SST climatology and variability. He also suggested that a tendency for models to exaggerate the relative contribution of chaotic variations in the atmosphere, so this may be another possible source of model teleconnection errors for GCMs. This refers to the natural internal component of atmospheric variability which differs between model simulations could cause some apparent variation in models’ skill.

5 Conclusion

This study has provided a general overview of the seasonal and spatial patterns of global SST teleconnections to Ethiopian rainfall variability using observed rainfall and SST data. It has also evaluated the ability of the HadGEM2 and HadGEM3-GA3.0 coupled atmosphere–ocean Global Circulation Models (AOGCMs) to simulate seasonal SST teleconnections to rainfall at the subnational scale, using Ethiopia and these two models as a case study. A quasi-objective method was employed to define coherent seasons and regions of SST-rainfall teleconnections for Ethiopia. We produced maps of the local correlations from five SST indices—representing the main tropical modes of variability—to gridded monthly and seasonal rainfall over Ethiopia. Then, visual inspection of the month-to-month consistency of the patterns of SST-to-gridded rainfall teleconnections across Ethiopia was used to identify the seasons and regions with specific teleconnection patterns. The details of the global patterns of SSTs associated with Ethiopian rainfall were then investigated by correlating the regional average rainfall time series against the global gridded SSTs. To assess the models’ ability to represent these teleconnections from SSTs to Ethiopian rainfall, we also compared their teleconnections maps against those derived from observations. The main findings of this study are summarised as follows.

We find there are three distinct rainfall seasons in Ethiopia with their specific SST-to-rainfall teleconnection patterns. These are March–May (MAM), July–September (JAS) and October–November (ON). Note that December rainfall has very little correlation with SSTs. Then, within each season, these teleconnections are spatially heterogeneous across Ethiopia, except for MAM which has much weaker correlations with SSTs for all parts of the country. Results for the JAS rainfall season (the Main Rains over most of the country except southern Ethiopia) confirm

those of other studies, such as the negative association with Niño3.4. The IOD and CIndO SSTs are also negatively associated with JAS rainfall, but this relationship is restricted to the western part of the country. The Small Rainfall season (ON) is also analysed here, and results show that conversely the southern part of Ethiopia is positively associated with Niño3.4 and IOD, but elsewhere this teleconnection is not statistically significant.

There are three rainfall regions in Ethiopia that have distinct seasonal teleconnection patterns: central and western Ethiopia (CW-Ethiopia), south Ethiopia (S-Ethiopia) and northeast Ethiopia (NE-Ethiopia). Over CW-Ethiopia, JAS rainfall is significantly and negatively correlated with the Niño3.4, CIndO and IOD modes of SST variability. The second one is the S-Ethiopian Region, where its Small Rainfall season (ON) is positively and significantly related to Niño3.4 and the IOD. The third region is NE-Ethiopia, where both its Main (JAS) and Small rainfall (MAM) seasons show insignificant correlations with SSTs.

We found that both the HadGEM2 and HadGEM3-GA3.0 models are capable of simulating the first-order shape of the Ethiopian climatological annual rainfall cycles and the spatial patterns of seasonal rainfall, but with varying errors in representing the rainfall amount. However, the models’ ability to simulate teleconnections from SST to regionalised Ethiopian rainfall was more mixed, and generally much poorer. Only the IOD to S-Ethiopia ON rainfall teleconnection in the HadGEM2 and HadGEM3-GA3.0 (N96) models is represented quite well. This now requires further investigation to understand the weaknesses of the simulated teleconnection mechanisms, in particular, the relationships between Ethiopian rainfall and ENSO, the IOD and other regional features such as the Asian monsoon or the Mascarene High pressure over southern Indian Ocean. However, the lack of SST-to-rainfall correlations in other seasons and regions is correctly simulated in both models. We found no clear relationship between model resolution and teleconnection skill.

Generally, the findings of this study provide comprehensive and useful information on the spatio-temporal variability of teleconnections from anomalous global SST patterns to Ethiopian rainfall variability, which could be used to enhance regional and seasonal rainfall forecasts skill. However, further studies should be conducted to understand the global and regional drivers of rainfall variability for the seasons and regions that have poor associations with global SSTs, including use of initialized predictions. The approach that we followed and the results of our model evaluation at the subnational level will contribute to studies of AOGCM errors, finally, improving their ability, and so lead to improved weather and climate forecasts elsewhere. It also provides a methodology to

validate the performance of a wider range of models that could be used for scientific study and operational activities.

Acknowledgments MAD and DPR were supported by U.K. Department for International Development (DFID)-Met Office Hadley Centre Climate Science Research Partnership (CSRP) program, Agreement Number: L0830. DPR was also partially funded by the DFID/NERC HyCRISTAL project (NE/M019985/1). The views expressed are not necessarily those of DFID. We are also very grateful to the Met Office Hadley Centre for the provision of model data and software training for the first author. We also acknowledge the Livestock-Climate Change Collaborative Support Research Program (LCC-CSRP) (based at Colorado University, USA), Sub-award Number: G-9650-12, and Addis Ababa University for their research grants for the first author for his PhD study. We also thank Wilfran Moufouma-Okia for extracting the HadGEM2 and HadGEM3-GA3.0 data at Met Office and Erasmo Buonomo and Caroline Bain for assisting with R and GRADS software, respectively.

Open Access This article is distributed under the terms of the Creative Commons Attribution 4.0 International License (<http://creativecommons.org/licenses/by/4.0/>), which permits unrestricted use, distribution, and reproduction in any medium, provided you give appropriate credit to the original author(s) and the source, provide a link to the Creative Commons license, and indicate if changes were made.

References

- Behera SK, Yamagata T (2003) Influence of the Indian Ocean dipole on the Southern Oscillation. *J Met Soc Jpn* 81:169–177. doi:10.2151/jmsj.81.169
- Black E, Slingo J, Sperber KR (2003) An observational study of the relationship between excessively strong short rains in coastal east Africa and Indian Ocean SST. *Mon Weather Rev* 131:74–94. doi:10.1175/1520-0493
- Camberlin P, Janicot S, Pocard I (2001) Seasonality and atmospheric dynamics of the teleconnection between African rainfall and tropical sea-surface temperature: Atlantic versus ENSO. *Int J Climatol* 21:973–1005. doi:10.1002/joc.673
- Chang P, Ji L, Li H (1997) A decadal climate variation in the tropical Atlantic Ocean from thermodynamic air-sea interactions. *Nature* 385:516–518. doi:10.1038/385516a0
- Cheung WH, Senay G, Singh A (2008) Trends and spatial distribution of annual and seasonal rainfall in Ethiopia. *Int J Climatol* 28:1723–1734. doi:10.1002/joc.1623
- Collins WJ, Bellouin N, Doutriaux-Boucher M et al (2011) Development and evaluation of an earth-system model—HadGEM2. *Geosci Model Dev* 4:1051–1075. doi:10.5194/gmd-4-1051-2011
- Conway D, Lisa E, Schipper F (2011) Adaptation to climate change in Africa: challenges and opportunities identified from Ethiopia. *Global Environ Change* 21:227–237. doi:10.1016/j.gloenvcha.2010.07.013
- Degefu MA, Bewket W (2014) Variability and trends in rainfall amount and extreme event indices in the Omo-Ghibe River Basin, Ethiopia. *Reg Environ Change* 14:799–810. doi:10.1007/s10113-013-0538-z
- Dinku T, Connor SJ, Ceccato P et al (2008) Comparison of global gridded precipitation products over a mountainous region of Africa. *Int J Climatol* 28:1627–1638. doi:10.1002/joc.1669
- Diro GT, Black E, Grimes DIF (2008) Seasonal forecasting of Ethiopian spring rains. *Meteorol Appl* 15:73–83. doi:10.1002/met.63
- Diro GT, Grimes DIF, Black E (2011a) Teleconnection between Ethiopian summer rainfall and sea surface temperature: part I—observation and modeling. *Clim Dyn* 37:103–119. doi:10.1007/s00382-010-0837-8
- Diro GT, Grimes DIF, Black E (2011b) Teleconnections between Ethiopian summer rainfall and sea surface temperature: part II. Seasonal forecasting. *Clim Dyn* 37:121–131. doi:10.1007/s00382-010-0896-x
- Enfield DB, Mestas-Nunez AM, Mayer DA, Cid-Serrano L (1999) How ubiquitous is the dipole relationship in tropical Atlantic sea surface temperature? *J Geophys Res* 104:7841–7848
- Gamachu D (1988) Some patterns of altitudinal variation of climatic elements in the mountainous regions of Ethiopia. *MRD* 8:131–138. doi:10.2307/3673439
- Gissila T, Black E, Grimes DIF et al (2004) Seasonal forecasting of the Ethiopian summer rains. *Int J Climatol* 24:1345–1358. doi:10.1002/joc.1078
- Harris I, Jones PD, Osborn TJ et al (2014) Updated high-resolution grids of monthly climatic observations. *Int J Climatol* 34:623–642. doi:10.1002/joc.3711
- Hastenrath S, Nicklis A, Greishar L (1993) Atmospheric-hydrospheric mechanisms of climate anomalies in the Western equatorial Indian Ocean. *J Geophys Res* 98:219–235. doi:10.1029/93JC02330
- Hewitt HT, Copey D, Culverwell ID et al (2011) Design and implementation of the infrastructure of HadGEM3: the next-generation Met Office climate modelling system. *Geosci Model Dev* 4:223–253. doi:10.5194/gmd-4-223-2011
- Jury MR, Funk C (2012) Climatic trends over Ethiopia: regional signals and drivers. *Int J Climatol* 33:1924–1935. doi:10.1002/joc.3560
- Kassahun B (1987) Weather systems over Ethiopia. In: *Proceedings of First Tech. Conf. on Meteorological Research in Eastern and Southern Africa*. Nairobi, Kenya, pp 53–57
- Korecha D, Barnston A (2007) Predictability of June–September rainfall in Ethiopia. *Mon Weather Rev* 135:628–650. doi:10.1175/MWR3304.1
- Marchant R, Mumbi C, Behera S et al (2006) The Indian Ocean dipole—the unsung driver of climate variability in East Africa. *Afr J Ecol* 45:4–16. doi:10.1111/j.1365-2028.2006.00707.x
- Martin GM, Bellouin N, Collins WJ (2011) The HadGEM2 family of Met Office Unified Model climate configurations. *Geosci Model Dev* 4:723–757. doi:10.5194/gmd-4-723-2011
- Mitchell TD, Jones PD (2005) An improved method of constructing a database of monthly climate observations an associated high-resolution grids. *Int J Climatol* 25:693–712
- Nicholson SE, Kim J (1997) The relationship of the El Niño southern oscillation to African rainfall. *Int J Climatol* 17:117–135. doi:10.1002/(SICI)1097-0088(199702)17<117:AID-JOC84>3.0.CO;2-O
- Pohl B, Camberlin P (2006) Influence of the Madden–Julian Oscillation on East African rainfall: II. March–May season extremes and interannual variability. *Q J R Meteorol Soc* 132:2541–2558. doi:10.1256/qj.05.223
- Rayner NA, Parker DE, Horton EB et al (2003) Global analyses of sea surface temperature, sea ice, and night marine air temperature since the late nineteenth century. *J Geophys Res* 108(D14):4407. doi:10.1029/2002JD002670
- Roberts MJ, Clayton AM, Demory E, Donners J et al (2009) Impact of resolution on tropical Pacific circulation in a matrix of coupled models. *J Climate* 22:2541–2556. doi:10.1175/2008JCLI2537.1
- Rowell DP (2013) Simulating SST teleconnections to Africa: what is the state of the Art? *J Climate* 26:5397–5418. doi:10.1175/JCLI-D-12-00761.1

- Saji HN, Yamagata T (2003) Structure of SST and surface wind variability in COADS observations during IOD years. *J Climate* 16:2735–2751. doi:[10.1175/1520-0442\(2003\)016](https://doi.org/10.1175/1520-0442(2003)016)
- Saji NH, Goswami BN, Vinayachandran PN et al (1999) A dipole mode in the tropical Indian Ocean. *Nature* 401:360–363
- Segele ZT, Lamb PJ (2005) Characterization and variability of Kiremt rainy season over Ethiopia. *Meteorol Atmos Phys* 89:153–180. doi:[10.1007/s00703-005-0127-x](https://doi.org/10.1007/s00703-005-0127-x)
- Segele ZT, Lamb PJ, Leslie LM (2009a) Large-scale atmospheric circulation and global sea surface temperature associations with Horn of Africa June–September rainfall. *Int J Climatol* 29:1075–1100. doi:[10.1002/joc.1751](https://doi.org/10.1002/joc.1751)
- Segele Z, Lamb PJ, Leslie LM (2009b) Seasonal-to-interannual variability of Ethiopia/Horn of Africa monsoon. Part I: associations of Wavelet-Filtered large-scale atmospheric circulation and global sea surface temperature. *J Climate* 22:3396–3421. doi:[10.1175/2008JCLI2859.1](https://doi.org/10.1175/2008JCLI2859.1)
- Seleshi Y, Zanke U (2004) Recent changes in rainfall and rainy days in Ethiopia. *Int J Climatol* 24:973–983. doi:[10.1002/joc.1052](https://doi.org/10.1002/joc.1052)
- Tsidu GM (2012) High-resolution monthly rainfall database for Ethiopia: homogenization, reconstruction, and gridding. *J Climate* 25:8422–8443. doi:[10.1175/JCLI-D-12-00027.1](https://doi.org/10.1175/JCLI-D-12-00027.1)
- Ummenhofer CC, Sen Gupta A, England MH (2009) Contribution of Indian Ocean sea surface temperatures to enhance east African rainfall. *J Climate* 22:993–1013. doi:[10.1029/2009GL038416](https://doi.org/10.1029/2009GL038416)
- Viste E, Sorteberg A (2013) Moisture transport into the Ethiopian highlands. *Int J Climatol* 33:249–263. doi:[10.1002/joc.3409](https://doi.org/10.1002/joc.3409)
- Zaroug MAH, Eltahir EAB, Giorgi F (2014a) Droughts and floods over the upper catchment of the Blue Nile and their connections to the timing of El Niño and La Niña events. *Hydrol Earth Syst Sci* 18:1239–1249. doi:[10.5194/hess-18-1239-2014](https://doi.org/10.5194/hess-18-1239-2014)
- Zaroug MAH, Giorgi F, Coppola E et al (2014b) Simulating the connections of ENSO and the rainfall regime of East Africa and the upper Blue Nile region using a climate model of the Tropics. *Hydrol Earth Syst Sci* 18:4311–4323. doi:[10.5194/hess-18-4311-2014](https://doi.org/10.5194/hess-18-4311-2014)